

Evolution of interfaces for a model interpolating between diffusion-limited aggregation and the Eden model

Pierre Devillard and H. Eugene Stanley

Center for Polymer Studies and Department of Physics, Boston University, Boston, Massachusetts 02215

(Received 31 May 1988; revised manuscript received 26 October 1988)

We study the evolution of interfaces for a generalization of a diffusion-limited aggregation process in two dimensions, where the walkers are launched from any unoccupied site and have a lifetime τ . For $\tau=1$, the model reduces to variant *B* of the Eden model. However, Eden model *B* does not respond to noise reduction in the same way as the other forms of the Eden model (*A* and *C*). As τ increases, stable cellular patterns emerge that resemble the patterns in directional solidification.

I. INTRODUCTION

There have been numerous studies of the surface of the Eden model in various space dimensions d .¹⁻¹¹ We restrict ourselves to the two-dimensional (2D) case in the "strip geometry." We start from a one-dimensional line of length L of seed particles on a square lattice; periodic boundary conditions are used on the sides of the strip.

Although the Eden model produces nonfractal clusters, the surfaces are fractal. The usual definition of the surface width is

$$w \equiv \left[\frac{1}{N} \sum_{i=1}^N (h_i - \langle h \rangle)^2 \right]^{1/2}, \quad (1a)$$

where N is the number of perimeter sites, h_i the y coordinate of the perimeter site i , and $\langle h \rangle$ the mean height,

$$\langle h \rangle \equiv \frac{1}{N} \sum_{i=1}^N h_i. \quad (1b)$$

The time t is chosen to be the mass of the cluster and w is a function of t and L . Since $\langle h \rangle \sim t/L$, we can write $w = w(\langle h \rangle, L)$. $w(\langle h \rangle, L)$ obeys the scaling relationship¹⁰

$$w \sim L^\chi f \left(\frac{\langle h \rangle}{L^z} \right), \quad (2)$$

where $z = \frac{3}{2}$ and $\chi = \frac{1}{2}$ exactly⁵ for the 2D Eden model. However, large crossover regions and finite-size effects make direct numerical computations of the exponent z difficult. If noise reduction is used,¹² then these large crossover regions become smaller and the exponents z and χ can be obtained much more easily.^{13,14}

The width of diffusion-limited aggregation¹⁵ (DLA) in strip geometry has also been extensively studied.¹⁶⁻¹⁸ In contrast to the Eden model, DLA growth is governed by a diffusion field and proceeds in a nonlocal fashion. We study the roughening of the surface for a variation of a model previously introduced in Refs. 19 and 20 which interpolates between DLA deposition and the Eden model. In regular DLA deposition,¹⁶⁻¹⁸ the principle is to send walkers from infinity; when the walker touches a perimeter site, this perimeter site becomes part of the cluster.²¹ In this model, one launches a walker from any empty lattice site. The number of time steps the random walker has

performed is recorded. If the walker touches the cluster before τ time steps, then the *previously visited* perimeter site becomes a cluster site [this is the dielectric breakdown (DBM) boundary condition].¹² If the walker has not touched the cluster after time τ , it is killed and another random walker is launched from an empty site chosen at random. Thus a walker starting from a distance greater than τ from the cluster will always be killed before touching the cluster. In fact, most of the walkers that will touch the cluster will have been launched in a layer of thickness of order $\sqrt{\tau}$ from the perimeter of the cluster.

In our simulations, we chose a site at random in the launch strip defined as follows. The ordinate of the bottom line of the strip is the highest ordinate such that *all sites* below that line are occupied. The ordinate of the top line of the launch strip is $h_{\max} + \tau + 1$ where h_{\max} is the highest point of the cluster. If the site chosen in this launch strip happens to be occupied, then another site is chosen until an empty (and thus acceptable) site has been found. This is equivalent to choosing a walker at random anywhere except on the cluster and allowing it to walk until it touches the cluster or dies.

II. SCALING BEHAVIOR FOR $\tau=1$

For $\tau=1$, the only way the cluster can grow is when a walker is created on a perimeter site and steps on the cluster at the first time step. Open bonds are defined as bonds that join a cluster site to a perimeter site. In variant *B* of the Eden model,⁴ an open bond is chosen at random and the corresponding perimeter site is occupied. Consequently, for $\tau=1$, our model reduces to variant *B* of the Eden model. Some perimeter sites are more likely to grow than others, but the ratio of the *maximum* probability for a perimeter site to become a cluster site to the *minimum* probability is *bounded from above* (Fig. 1). The "active perimeter" P_{\max} is defined as the inverse of the maximum growth probability Π_{\max} . By definition, d_{\max} , the fractal dimension of the active perimeter, is defined as $P_{\max} \sim t^{d_{\max}}$. Using Refs. 22 and 23, we have $d_f = 1 + d_{\max}$. Here $d_{\max} = 1$, since the maximum growth probability scales as L^{-1} . Hence, the present model has fractal dimension $d_f = 2$.

Since the calculation of the exponents z and χ [Eq. (2)]

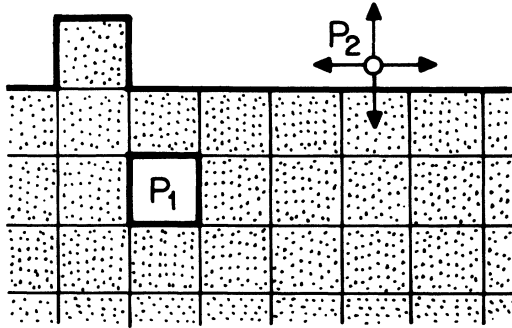


FIG. 1. The shaded sites are the cluster sites. In this model, perimeter site P_1 is four times more likely to grow than perimeter site P_2 which has only one nearest neighbor occupied. For the Eden model A , P_1 and P_2 have equal growth probability.

is hampered by large corrections to scaling, we applied noise reduction. Figure 2 shows w as a function of time for $\tau=1$, $L=4000$, and $s=3$, where s denotes the noise-reduction parameter (the number of times a given perimeter site must be chosen to be occupied before it actually is allowed to become occupied). First, when t is less than a few times L , we do not get scaling. In this time region, when the noise-reduction parameter s is more than 10, we obtained oscillations corresponding to the filling of layers.¹⁴ Then, there is a scaling region $t_1 < t < t_2$ where $w \sim t^\beta$. From Eq. (1), $\beta = \chi/z$ follows. For $s=4$, we obtained $\beta = 0.32 \pm 0.03$ after averaging over 20 samples. At large time, w saturates and we denote by W the limit of the width as $t \rightarrow \infty$: $W(L,s) \equiv \lim_{t \rightarrow \infty} w(t,L,s)$.

We now turn to the evaluation of χ . Figure 3 shows the saturation width W as a function of the width of the strip L for various values of the noise-reduction parameter s . We obtained for $s=3$, $\chi = 0.50 \pm 0.02$ and for $s=10$, $\chi = 0.50 \pm 0.10$. Thus, variant B of the Eden model seems, at first sight, to behave like the other variants of the Eden model.

Let us examine now what happens when the noise-reduction is incorporated in the scaling. The scaling of the width for models A and C (Ref. 14) was shown to be

$$w^2(t,L,s) \approx [a(s)L^\chi F(tL^{-z}s^{-y})]^2 + w_i^2(s), \quad (3)$$

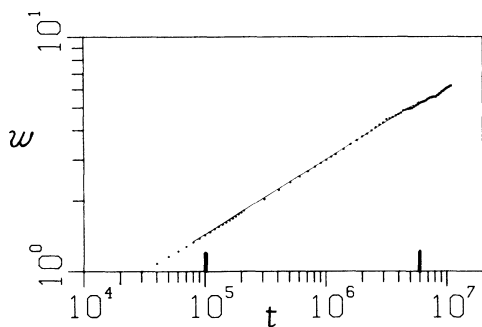


FIG. 2. Log-log plot of w as a function of time for $L=4000$, $\tau=1$, and $s=3$ after averaging over 20 samples. The quantity $\beta_{\text{eff}} = \partial \log w / \partial \log t$ first increases, then remains constant in the range $10^5 < t < 6 \times 10^6$ and finally decreases as w goes toward saturation. The straight line is a fit in the range of constant β_{eff} , limited by the two heavy bars. We find $\beta = 0.32 \pm 0.03$.

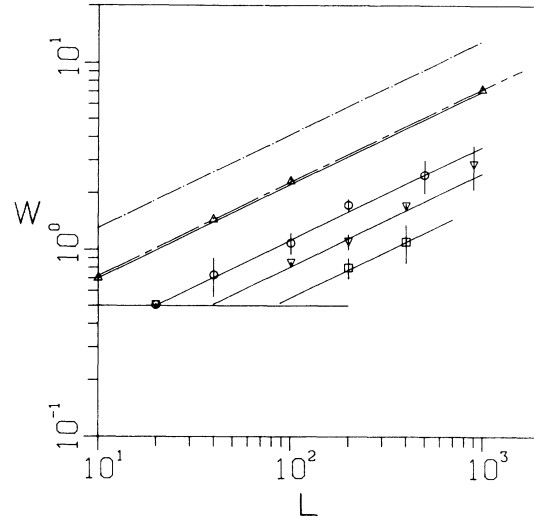


FIG. 3. Log-log plot of W as a function of L for model B for various values of the noise reduction parameters: $s=3$ (Δ), $s=10$ (\circ), $s=20$ (∇), and $s=40$ (\square). For model B , we obtained: $\chi = 0.5 \pm 0.03$ for $s=3$, $\chi = 0.5 \pm 0.12$ for $s=10$. The upper dashed line are data for $s=1$ from Ref. 8 for model A . The lower dashed line is the formula obtained for s very large by Wolf and Kertész (Ref. 14) for models A and C . The heavy straight lines of slope $\frac{1}{2}$ are a guide to the eye and not a fit to the data. The heavy horizontal line is the plateau $W=0.5$.

where w_i is the intrinsic width (and does not depend on L) and y an exponent close to 1. F is a scaling function, and $a(s)$ is given by $a(s) \approx \sqrt{1 + 2.3/s}$. As s increases, w_i decreases and tends to zero as s becomes very large. In models A and C , noise reduction introduces time rescaling. Consider w as a function of t for fixed L . The time t_1 for which the scaling region begins increases with s (as s^ν). In variant B we also observed this effect.

However, in models A and C , for L fixed, when s is increased, larger and larger times are required to reach the saturation regime ($t_2 \rightarrow \infty$ as $s \rightarrow \infty$). For model B , this is not the case, because, in addition to rescaling the time, noise reduction also reduces the saturation width $W(L,s)$. If (3) was also applicable to variant B , we would have, since $\chi = \frac{1}{2}$,

$$\frac{W^2(L,s)}{L} = a^2(s)F_\infty^2 + \frac{w_i^2(s)}{L}, \quad (4)$$

where $F_\infty = \lim_{x \rightarrow \infty} F(x)$. To test Eq. (4), we plotted in Fig. 4 W^2/L as a function of $1/s$. We obtain a straight line but, contrary to the findings of Ref. 14, the extrapolation to $s \rightarrow \infty$ seems to give 0. This means that $a(s)$ behaves as $1/\sqrt{s}$ in our version of variant B .

For $s = \infty$, the interface remains flat and the concept of saturation width is meaningless. However, it makes sense to consider the quantity

$$W_{AC}(L) = \lim_{s \rightarrow \infty} \lim_{t \rightarrow \infty} w(t,L,s)$$

in which the two limits do not commute.

For variants A and C , the quantity $W_{AC}(L)$ is given by the approximate formula^{13,14} $W_{AC}(L) \approx \sqrt{0.052} \times \sqrt{L}$. For any s , all the points $[W(s,L), L]$ lie above the line

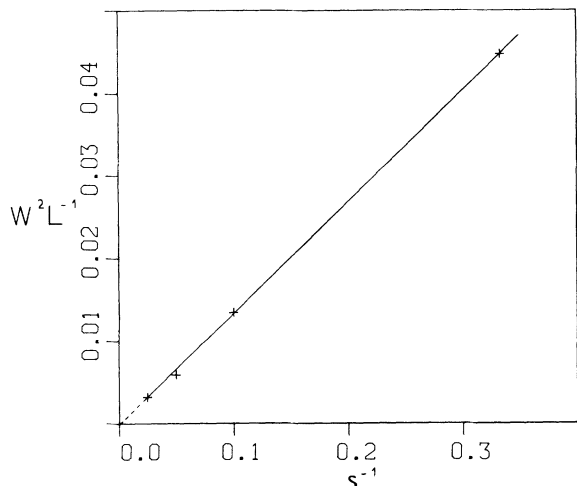


FIG. 4. Plot of W^2/L as a function of $1/s$ for $L=200$.

$W_{AC}(L) \approx \sqrt{0.052} \times \sqrt{L}$ [for L reasonably large such that Eq. (3) holds].

For variant B , this is not the case, as can be seen in Fig. 3. For $s \geq 3$, the points $[W(s,L), L]$ fall below the line $W_{AC}(L) \approx \sqrt{0.052} \times \sqrt{L}$. For large values of s , the curves $\log W$ as a function of $\log L$ have two parts. For $L < L^*$ there is a plateau at $W=0.5$. For $L > L^*$ there is a straight line of slope of $\sim \frac{1}{2}$. L^* tends to infinity as $s \rightarrow \infty$.

Thus, for variant B , we propose the scaling relation

$$W \sim g(L/s) \tag{5}$$

where $g(L/s) \sim (L/s)^{1/2}$ as $x \rightarrow \infty$ and $g(L/s) \sim \frac{1}{2}$ as

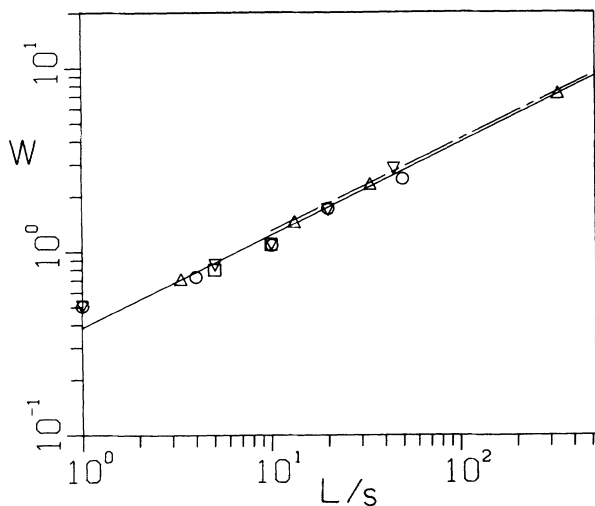


FIG. 5. Log-log plot of W as a function of L/s for values of $s=3$ (Δ), $s=10$ (\circ), $s=20$ (∇), and $s=40$ (\square). The upper dashed line corresponds to the results of Ref. 8 for model A and $s=1$. Our data seem to collapse on a single curve. For L/s greater than 10, this curve is almost a straight line of slope χ' , and the lower heavy line is a least-squares fit in this region. We find $\chi' = 0.50 \pm 0.03$.

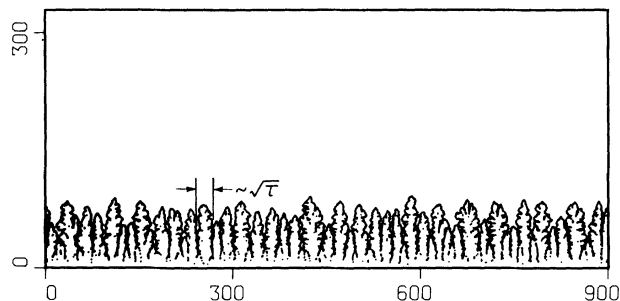


FIG. 6. "Cellular pattern" obtained for $L=901$, $s=10$, and $\tau=1000$ after $t=5 \times 10^4$. An approximate "wavelength" of order $\sqrt{\tau} \approx 30$ lattice units can be seen by eye.

$L/s \rightarrow 0$. Note that (5) implies $L^* \sim s$.

Since $W \sim \sqrt{L}$ for large L , one expects $\chi' = \chi = \frac{1}{2}$. Numerically, we obtained $\chi' = 0.5 \pm 0.02$. In order to test this assumption, we plot W as a function of L/s (Fig. 5). We find that the data obtained for values of s ranging from 1 to 40 fall approximately on a single curve. For L/s larger than 10, we have a scaling region where $g(L/s) \sim (L/s)^{\chi'}$. We obtained $\chi' = 0.50 \pm 0.02$.

III. BEHAVIOR FOR $\tau > 1$

When $1 \ll \sqrt{\tau} \ll L$, cellular patterns arise. Figure 6 shows such a pattern for $s=10$ and $\tau=1000$ at $t=50000$. Note that a wavelength of order $\sqrt{\tau}$ appears, i.e., the typical "cell" width is of order $\sqrt{\tau}$. Though the model studied here was not explicitly designed to describe the physics of directional solidification, the patterns obtained do strongly resemble directional solidification.²⁴⁻²⁶ However, in the simulations of Refs. 24-26, the random walkers have a bias, which also introduces an effective length. It is

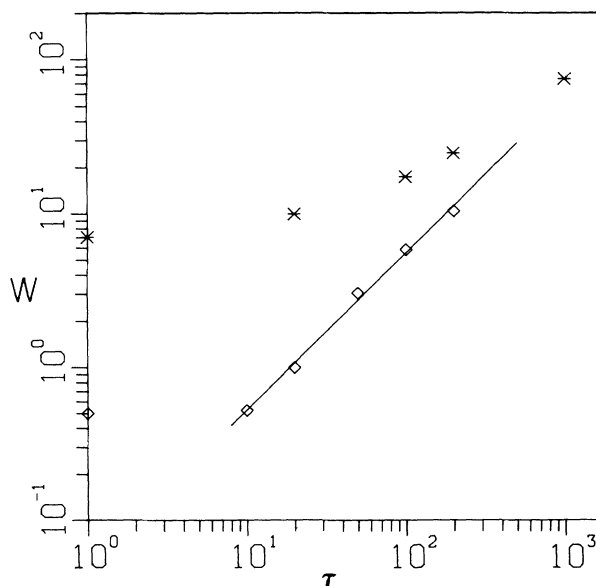


FIG. 7. Log-log plot of W vs τ [$s=1$, $L=301$ ($*$); $s=60$, $L=101$ (\diamond)]. For $\tau > 20$, we find $W \sim \tau^x$ with $x = 1.0 \pm 0.1$.

tempting to conclude that when a finite diffusion length is introduced in a DLA deposition process, cellular patterns are obtained.

As a function of time, the width increases and then saturates to a value W . For τ larger than 100, we had to modify our original algorithm since it would consume too much computer time and be very inefficient. The ordinate of the top line of the strip where we launch walkers was chosen to be $h_{\max} + 4\sqrt{\tau}$ instead of $h_{\max} + \tau + 1$. We checked that the results were not altered by changing this ordinate to $h_{\max} + 10\sqrt{\tau}$.

A plot of W as a function of τ (see Fig. 7) for different values of s shows that W increases with τ . When noise reduction is applied, a scaling region seems to emerge where $W \sim \tau^x$ with $x = 1.0 \pm 0.1$.

In the limit $\tau \rightarrow \infty$, the model should reduce to DLA. The fact that the walkers are launched from everywhere is immaterial since in the limit τ very large, most of the walkers that will contribute to the growth of the cluster will have been created far from the cluster.

IV. DISCUSSION AND CONCLUSIONS

The purpose of this study was to show that the introduction of noise reduction in Eden models can have different consequences on the scaling properties of the

width, depending on the variant considered. In this paper only $d=2$ is considered and the exponents χ and z are not changed by noise reduction (for s finite). However, we find that the scaling properties of the width with respect to s are model dependent (nonuniversal). The scaling law (3), which was found by Kertész and Wolf¹⁴ for both variants A and C , is somewhat different for variant B . For variant B , the width for large time W obeys a scaling law $W \sim g(L/s)$. The fact that we have counters on the perimeter sites might be the reason why our version of variant B responds to noise reduction in a way which is different from variants A and C . Our version leads to a new way of measuring the roughness exponent χ accurately. Finally, we show that, if in a diffusion-limited aggregation process the walkers have a finite lifetime, cellular patterns emerge with a characteristic wavelength given by the diffusion length.

ACKNOWLEDGMENTS

We would like to thank A. Aharony, A. Bunde, A. Coniglio, N. Jan, S. Redner, D. Stauffer, and R. Swendsen for useful discussions. We are greatly indebted to J. Kertész for his suggestions and advice. The Center for Polymer Studies is supported by grants from the National Science Foundation and the Office of Naval Research.

- ¹M. Eden, in *Proceedings of the Fourth International Symposium on Mathematical Statistics and Probability, Berkeley, 1961*, edited by F. Neyman (Univ. of California Press, Berkeley, 1961), Vol. 4, p. 223.
- ²M. Plischke and Z. Rácz, *Phys. Rev. Lett.* **53**, 415 (1984).
- ³R. Jullien and R. Botet, *J. Phys. A* **18**, 2279 (1985).
- ⁴M. Plischke and Z. Rácz, *Phys. Rev. A* **32**, 3825 (1985).
- ⁵M. Kardar, G. Parisi, and Y. C. Zhang, *Phys. Rev. Lett.* **56**, 889 (1986).
- ⁶M. Plischke, Z. Rácz, and D. Liu, *Phys. Rev. B* **35**, 3485 (1987).
- ⁷D. Dhar, poster at *Statistical Physics: Invited Lectures from Statphys 16*, Proceedings of the Sixteenth (IUPAP) International Conference on Thermodynamics and Statistical Mechanics (STATPHYS-16), Boston, 1986, edited by H. E. Stanley (North-Holland, Amsterdam, 1986).
- ⁸J. G. Zabolitzky and D. Stauffer, *Phys. Rev. A* **34**, 1523 (1986).
- ⁹D. Stauffer in *Percolation Theory and Ergodic Theory of Infinite Particle Systems*, edited by H. Kesten (Springer, Heidelberg, 1987).
- ¹⁰F. Family and T. Vicsek, *J. Phys. A* **18**, L75 (1985).
- ¹¹R. Hirsch and D. E. Wolf, *J. Phys. A* **19**, L251 (1986).
- ¹²C. Tang, *Phys. Rev. A* **31**, 1977 (1985); J. Nittmann and H. E. Stanley, *Nature* **321**, 663 (1986); J. Kertész and T. Vicsek, *J. Phys. A* **19**, L257 (1986).
- ¹³D. E. Wolf and J. Kertész, *J. Phys. A* **20**, L257 (1987).
- ¹⁴J. Kertész and D. E. Wolf, *J. Phys. A* **21**, 747 (1988).
- ¹⁵T. A. Witten and L. M. Sander, *Phys. Rev. Lett.* **47**, 1400 (1981).
- ¹⁶P. Meakin and F. Family, *Phys. Rev. A* **34**, 2558 (1986).
- ¹⁷Z. Rácz and T. Vicsek, *Phys. Rev. Lett.* **51**, 2382 (1983).
- ¹⁸P. Meakin, *Phys. Rev. B* **30**, 4207 (1984).
- ¹⁹K. A. Suresh, J. Nittmann, and F. Rondelez, *Europhys. Lett.* (to be published).
- ²⁰H. E. Stanley and J. Nittmann (unpublished).
- ²¹In fact, the way it is implemented to yield a computationally efficient algorithm is somewhat different and can be found in, R. C. Ball, R. M. Brady, G. Rossi, and B. R. Thompson, *Phys. Rev. Lett.* **55**, 1406 (1985); P. Meakin, in *On Growth and Form*, edited by H. E. Stanley and N. Ostrowsky (Nijhoff, Dordrecht, 1985).
- ²²L. A. Turkevich and H. Scher, *Phys. Rev. Lett.* **55**, 1026 (1985).
- ²³F. Leyvraz, *J. Phys. A* **18**, L941 (1985).
- ²⁴S. K. Sarkar and M. H. Jensen, *Phys. Rev. A* **35**, 1877 (1987).
- ²⁵T. Vicsek, *Phys. Rev. A* **32**, 3084 (1985).
- ²⁶J. Szép, J. Cserti, and J. Kertész, *J. Phys. A* **18**, L413 (1985).